Development of an incoherent broad-band cavity-enhanced aerosol extinction spectrometer and its application to measurement of aerosol optical hygroscopicity

WEIXIONG ZHAO,[1,4,*] XUEZHE XU,[1,2,4] BO FANG,[1,4] QILEI ZHANG,[1,2,4] XIAODONG QIAN,[1,2,4] SHUO WANG,[1,2,4] PAN LIU,[1,2,4] WEIJUN ZHANG,[1,2,3,4,*] ZHENZHU WANG,[4] DONG LIU,[4] YINBO HUANG,[4] DEAN S. VENABLES,[5] WEIDONG CHEN[6]

[1]*Laboratory of Atmospheric Physico-Chemistry, Anhui Institute of Optics and Fine Mechanics, Chinese Academy of Sciences, Hefei, 230031, Anhui, China*
[2]*Graduate School, University of Science and Technology of China, Hefei, 230026, Anhui, China*
[3]*School of Environmental Science and Optoelectronic Technology, University of Science and Technology of China, Hefei, 230026, Anhui, China*
[4]*Key Laboratory of Atmospheric Composition and Optical Radiation, Anhui Institute of Optics and Fine Mechanics, Chinese Academy of Sciences, Hefei 230031, Anhui, China*
[5]*Department of Chemistry and Environmental Research Institute, University College Cork, Cork, Ireland*
[6]*Laboratoire de Physicochimie de l'Atmosphère, Université du Littoral Côte d'Opale, 16 59140 Dunkerque, France*
**Corresponding author: wxzhao@aiofm.ac.cn; wjzhang@aiofm.ac.cn*

Received XX Month XXXX; revised XX Month, XXXX; accepted XX MonthXXXX; posted XX Month XXXX (Doc. ID XXXXX); publishedXX Month XXXX

We report on the development of a blue light-emitting diode (LED) based incoherent broad-band cavity-enhanced absorption spectroscopy (IBBCEAS) instrument for the measurement of the aerosol extinction coefficient at λ = 461 nm. With an effective absorption pathlength of 2.8 km, an optimum detection limit of 0.05 Mm^{-1} (5×10^{-10} cm^{-1}) was achieved with an averaging time of 84 s. The baseline drift of the developed spectrometer was about ± 0.3 Mm^{-1} over 2.5 h (1σ standard deviation). The performance of the system was evaluated with laboratory generated monodispersed polystyrene latex (PSL) spheres. The retrieved complex refractive index (CRI) of PSL agreed well with previously reported values. The relative humidity (RH) dependence of the aerosol extinction coefficient was measured using IBBCEAS. The measured extinction enhancement factor f(RH) values for 200 nm dry ammonium sulphate particles at different RH were in good agreement with the modeled values. Field performance of the aerosol extinction spectrometer was demonstrated at the Hefei Radiation Observatory (HeRO) site.© 2016 Optical Society of America

OCIS codes: *(010.1120) Air pollution monitoring; (010.1100) Aerosol detection; (120.6200) Spectrometers and spectroscopic instrumentation.*

http://dx.doi.org/xxxx

1. INTRODUCTION

Rapid urbanization and economic development has brought about serious environmental problems in the megacities of China. Concentrations of fine particles in the air of some Chinese cities, such as Beijing, often greatly exceed World Health Organization recommendations [1]. Atmospheric aerosols, liquid or solid particles suspended in the gaseous medium, are believed to be primarily responsible for the degradation of visibility [2-5]. The relationship between the visual range (L_v, conventionally in unit of km) and extinction coefficient (α_{ext}) at λ = 550 nm (conventionally in unit of Mm^{-1}, 1 Mm^{-1}= 10^{-8} cm^{-1}) can be described with Köschmeider equation [6]:

$$L_v = 3.912\times10^{-3}/\alpha_{ext,550nm}. \quad (1)$$

Depending on the ambient relative humidity (RH), since aerosol particles can take up water and they can become larger grow in size, leading to dramatic changes in light extinction, the extinction enhancement factor *f*(RH) is therefore a key parameter in assessing the aerosol effects on regional air quality, atmospheric visibility, and radiative transfer [7-12]. The extinction enhancement factor is defined as:

$$f(RH,\lambda) = \alpha_{ext}(RH,\lambda)/\alpha_{ext}(Dry,\lambda). \quad (2)$$

where α_{ext} (RH,λ) is the extinction coefficient at a defined RH (typically 85%), and α_{ext} (Dry,λ) is the corresponding dry extinction coefficient, where RH is smaller than 40%.

The aerosol extinction coefficient can be directly measured with a single-pass [13, 14] or multi-pass [15-17] extinction cell, and more recently by cavity-enhanced or cavity ring-down spectroscopy [18-32]. Further details can be found in some review papers [33-35]. The achievable detection limit of extinction cells is typically about 10 Mm^{-1}, limited by the absorption pathlength, which makes it is of practical use only for laboratory-generated aerosols or near-source aerosol plumes in the ambient atmosphere.

Cavity-enhanced and cavity ring-down spectroscopy use high-finesse optical cavities (stable optical resonators with high reflectivity mirrors) [36] to realize long effective absorption path lengths (up to several kilometers) in a compact resonant cavity (with a base length of ~ 1 m). These approaches, are highly sensitive (better than 0.1 Mm^{-1}), and accurate (< 3%), and are suited to real time, in-situ measurement of ambient aerosol extinction. Unlike other approaches, the nature suspended state of aerosol is not changed during the measurement. Both cavity-enhanced and cavity ring-down spectroscopy are well-established methods and are now among the most widely used spectroscopy techniques for extinction measurement.

However, most cavity based spectrometers operate at a single-wavelength and are susceptible to interferences from gas-phase absorption that also contribute to the measured extinction. Under this condition, extinction measurement with a single instrument is not enough : a second instrument or a second gas-phase reference channel for simultaneous measurement of gases absorption is required to compensate for the influence of gas absorption induced optical extinction. In 2011, Langridge et al. [37] described on the design and performance of an aircraft instrument utilizing an 8-channel cavity ring-down spectrometer for the aerosol extinction measurement : 3 of which channels were used for the measurement of dry extinction coefficients (RH = 10%) at λ = 405, 532, and 662 nm, 2 channels were used for the measurement of extinction coefficients at RH = 70%, and 95% at λ = 532 nm, and another 3 additional channels at λ = 405, 532, and 662 nm were used to account for gas absorption.

Incoherent broad-band cavity-enhanced absorption spectroscopy (IBBCEAS), first demonstrated by Fiedler et al. [38], is a class of methods combining high-finesse optical cavities with incoherent broad-band light sources, and has recently been widely adopted for trace gases and aerosol extinction measurement [39]. The detection sensitivity of IBBCEAS is comparable with typical CRDS methods. In 2009, Varma et al. [40] developed a 20 m long optical cavity for aerosol light extinction measurement between 630 – 690 nm at the SAPHIR atmospheric simulation chamber, and an intercomparison study of this instrument with other two cavity-based spectroscopy has been performed [41]. The main advantages of the IBBCEAS method over other single-wavelength cavity-based absorption spectroscopy are:

(1) measurement of aerosol extinction is much less susceptible to interferences from gas absorption. The broad-band spectral information of IBBCEAS allows multiple absorbing species to be quantified simultaneously using a single instrument, and their contribution to the total sample extinction can be then removed [41-43]. This method has been deployed in field applications [44, 45].

(2) wavelength-resolved aerosol extinction cross-section over a broad spectral region can be measured directly using the IBBCEAS method. By combining the number concentrations measurement at different particle diameters, wavelength resolved complex refractive index (CRI, the only intrinsic optical property of a particle) can be retrieved [46-49], which provides a useful tool for studying the optical properties research of, for example, brown carbon [34] or secondary organic aerosols [35].

In this paper, we report on the developed of a compact blue LED based IBBCEAS spectrometer for aerosol extinction measurement around λ = 461 nm. The relative humidity (RH) dependence of aerosol extinction was measured with IBBCEAS method. The developed spectrometer was tested with laboratory generated aerosols and was deployed for ambient air *f*(RH) measurement in a suburban observation site.

2. EXPERIMENTAL SETUP

A schematic diagram of the IBBCEAS aerosol extinction spectrometer is shown in Fig. 1. A 5W blue LED (LedEngin LZ110B200) was used as broad-band light source. The manufacturer given peak and the full-width at half maximum (FWHM) values of the LED emission spectrum was 460 nm and ~ 25 nm, respectively. The LED was mounted on a Peltier heat sink, and controlled with laser diode current and temperature drivers to stabilize the light emission intensity. The LED light was coupled directly from the LED into a multimode fiber of 500 μm core diameter with a numerical aperture (NA) of 0.22 (Ocean Optics).The emerging light from the fiber was collimated with a SMA air-spaced doublet collimators (f = 34.74 mm, NA = 0.26) and then injected into a high-finesse optical cavity. A bandpass filter, centered at 450 nm with an FWHM of 40 nm (Thorlabs FB 450-40), was located in front of the cavity.

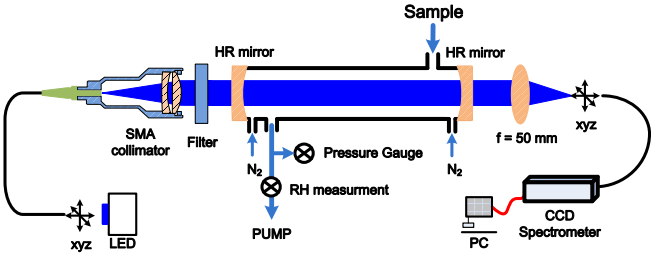

Fig. 1. Schematic diagram of the blue LED-based IBBCEAS aerosol optical extinction spectrometer.

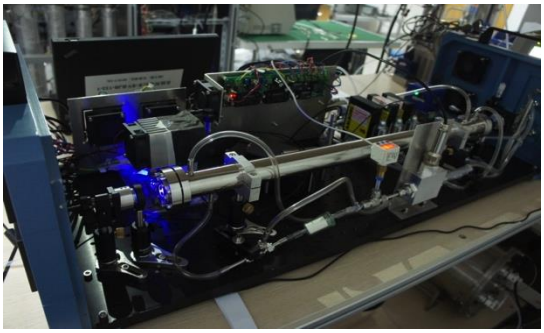

Fig. 2. Picture of the developed IBBCEAS aerosol extinction spectrometer.

The optical cavity was made of a 70 cm long polished stainless steel tube with an inner diameter of 35 mm, with two highly reflective mirrors at either end. The distance from the sample inlet to the outlet was about 56.6 cm. The sample flow (1.3 L/min) was controlled with a mass flow controller at atmospheric pressure. Purified dry filtered air at a flow rate of 100 ml/min was introduced near both mirrors to prevent mirror contamination by aerosol deposition. The temperature and relative humidity of the sample was measured with a hygrometer humidity sensor (Rotronic, model HC2) at the outlet of the cavity. Light transmitted through the cavity was collimated with a 50 mm focal

length achromatic lens, and coupled into a multi-mode optical fiber of 500 μm core diameter and 0.22 NA. The output of the fiber was directly connected to a CCD spectrometer (Ocean Optics Maya 2000 Pro, with a 100 μm slit width and a spectral resolution of 0.25 nm over the wavelength range of 411 - 497 nm). All the optical elements were assembled on a solid aluminum optical breadboard (102 cm long and 40 cm wide). A photograph of the aerosol extinction spectrometer is shown in Fig. 2.

3. RESULTS

3.1. Instrument Stability and Detection Limits

The mirror reflectivity R(λ) of the developed aerosol extinction spectrometer was determined from the Rayleigh scattering of N_2 and CO_2 [50] :

$$R(\lambda) = 1 - d\left(\frac{\left(I_{CO_2}(\lambda)/I_{N_2}(\lambda)\right)\sigma_{Ray}^{CO_2}(\lambda) - \sigma_{Ray}^{N_2}(\lambda)}{1 - I_{CO_2}(\lambda)/I_{N_2}(\lambda)}\right) \quad (3)$$

where d is the total cavity cell length, I_{CO2} (λ) and I_{N2} (λ) are the light intensities transmitted through the cavity with CO_2 and N_2, respectively. $\sigma_{Ray}^{CO_2}(\lambda)$ and $\sigma_{Ray}^{N_2}(\lambda)$ are the reference Rayleigh absorption cross-sections of CO_2 and N_2, respectively[51, 52]. The value of R_L (the ratio of d to the real cell length containing the sample when the cavity mirror is purged with filtered air) was determined from the absorption measurement of different NO_2 concentrations with and without mirror purging [43-45, 53]. The purge gas was turned off during the calibration of mirror reflectivity with N_2 and CO_2, and turned on during the measurement of aerosol extinction. A scale factor of 1.077 (1.4 L/1.3 L) was multiplied to the measurement result to account for dilution when the purge gas was on.

In this work, R(λ) at 461 nm (the wavelength corresponding to the peak value of the transmission spectrum of the cavity, which was used for data analyzing in this work) was determined to be 0.99979, and R_L was determined to be 1.18 (with an effective sample length of 59.3 cm), which led to an effective optical pathlength of about 2.8 km. The total uncertainty in the extinction measurement, with dominant contribution from the errors in R(λ) (~1%), R_L (~ 2%), and particle losses in the system (~2%, determined from measuring particle number concentrations at the inlet and outlet of the cavity with two condensation particle counters) [43, 44], was estimated to be 3%.

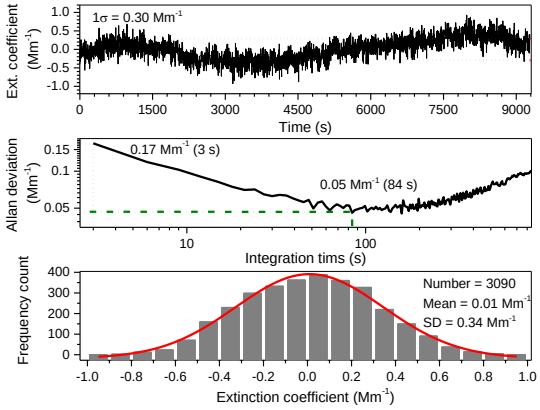

Fig. 3. Upper panel : time series measurement of particle-free zero air sample with a time resolution of 3 s at a wavelength of λ = 461 nm (long-term variation or stablity). Middle panel : Allan deviation plot of the extinction measurements. Lower panel : frequency distribution of the extinction measurement (short-term stability, or instrument precision).

The stability and detection sensitivity of the optical system was investigated using an Allan variance analysis, as shown in the middle panel of Fig. 3. Continuous time series measurement of particle-free zero air sample with a time resolution of 3 s (150 ms integrating time, and 20 spectra averaging) is shown in the upper panel of Fig. 3. Longer-term (2.5 h) base-line drift of the instrument was estimated to be ± 0.3 Mm^{-1} (1σ standard deviation). With 3 s averaging time, the detection sensitivity was 0.17 Mm^{-1}. For optimum detection performance, a minimum detection limit of 0.05 Mm^{-1} was attained with 84 s averaging time. This sensitivity is comparable with the state-of-the-art performance of extinction detection (0.02 Mm^{-1} with 10 s integration time) [25].

The frequency distribution of the extinction measurement is shown in the lower panel of Fig. 3. A Gaussian distribution was used for the histograms fit to obtain the mean and standard deviation (a measure of the instrument precision) of the particle-free zero air measurement. The corresponding confidence interval ($2\sigma n^{-1/2}$, where n is the number of data points) was 0.01 Mm^{-1}. The 1σ standard deviation of 0.34 Mm^{-1} of the histogram was consistent with the 1σ standard deviation of 0.30 Mm^{-1} determined from the continuous measurement shown in the upper panel, as would be expected.

3.2. Laboratory Results

The performance of the cavity-enhanced aerosol extinction spectrometer was evaluated using the measurement of laboratory-generated, NIST traceable monodispersed polystyrene latex (PSL) spheres with 6 different diameters. The method and the aerosol generation system were the same as reported in our previous work [43, 44]. Polydispersed aerosol were generated with TSI 3076 constant output atomizer, and then dried with a silica gel column dryer. After neutralizing with TSI 3077 aerosol neutralizer, size selected aerosol was generated by an electrostatic classifier (TSI differential mobility analyzer, 3080L) [43, 44].

Figure 4 shows the plot of the measured extinction coefficient versus the particle number concentrations for 200 nm, 240 nm, 300 nm, 350 nm, 400 nm, and 500 nm nonabsorbing PSL particles, respectively. The particle number concentrations were measured with a condensation particle counter (CPC 3776). The extinction cross-sections were derived from the slopes of the linear fits of the measured extinction coefficients to the measured particle number concentrations.

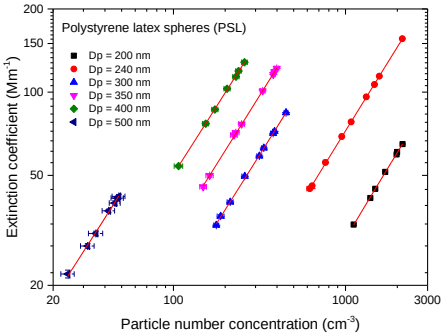

Fig. 4. Extinction coefficients as a function of particle number concentration at λ = 461 nm for PSL spheres at 200, 240, 300, 350, 400 and 500 nm diameters, respectively. The slope of each linear fit represents the extinction cross-section of each PSL size.

The extinction coefficient of particles are calculated based on [21]:

$$\alpha_{ext} = \int N(D)\frac{\pi}{4}D^2 Q_{ext}(m,x)dD. \qquad (4)$$

where $x = \pi D/\lambda$ is the size parameter, $m = n + ik$ is the CRI of the particle (where n and k correspond to light scattering and absorption by aerosol, respectively). N is the number of particles per unit volume in the size bin dD with mean diameter D, and $\pi/4D^2Q_{ext}(m,x)$ is the extinction cross section (σ_{ext}) and can be obtained from the ratio of the measured α_{ext} to particle number concentration ($\sigma_{ext} = \alpha_{ext}/N$, as shown in Fig. 4). For chemically homogeneous spherical particles, the extinction efficiency ($Q_{ext} = 4\sigma_{ext}/\pi D^2$) can be calculated from Mie theory.

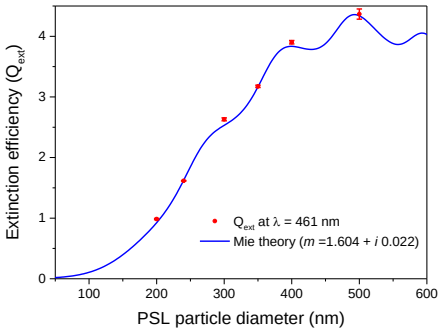

Fig. 5. The extinction efficiency (Q_{ext}) as a function of particle diameter for six different sizes PSL particle at λ = 461 nm.

A plot of the measured Q_{ext} (derived from Fig. 4) as a function of particle diameter is shown in Fig. 5. A merit function was used for the retrieval of CRI [43, 44]:

$$\chi^2(n,k) = \sum_{i=1}^{Num}\frac{\left(Q_{ext,measured} - Q_{ext\_cal}(n,k)\right)^2}{\Delta Q_i^2}. \qquad (5)$$

where ΔQ is the standard deviation of the measured Q values for each diameter particle. χ^2 was calculated for a wide range of n and k values. The best-fit result gives the lowest value of the merit function (χ_0^2). The values of n and k that satisfy $\chi^2 = \chi_0^2 + 2.298$ are considered as the 1σ upper and lower bound of the CRI [24, 26].

The retrieved CRI for PSL particles was $m = 1.604^{+0.002}_{-0} + i0.022^{+0.001}_{-0.004}$ at λ = 461 nm, which agreed well with the value (m =1.60±0.02 + i0.01±0.03) reported by Lang-Yona et al. with continuous wave cavity ring down aerosol spectrometer at λ = 532 nm [54], and the value (m = 1.633±0.05 + i0.000±0.005) reported by Washenfelder et al. with a similar IBBCEAS broadband cavity method at λ = 420 nm[46]. These results show that the laboratory performance of our extinction spectrometer is qualitatively and quantitatively comparable to CRDS instruments and other IBBCEAS instruments, confirming that the developed spectrometer is suitable for high sensitive and accuracy measurement of aerosol extinction.

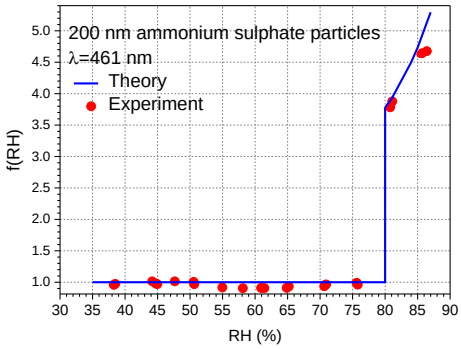

Fig. 6. RH dependence of extinction for 200 nm dry diameter ammonium sulphate particles.

The validation of the f(RH) measurement was performed with laboratory-generated ammonium sulfate (AS). The sample aerosol was generated using a constant output atomizer (TSI 3076) with purified compressed zero air, dried with a silica gel column dryer, and then neutralized with an aerosol neutralizer (TSI 3077) to obtain an equilibrium charge distribution. Size-selected 200 nm dry AS aerosol was selected with an electrostatic classifier (TSI 3080 differential mobility analyzer) and used to demonstrate the quantitative validity of the RH measurement. The test was performed by varying the relative humidity. A temperature controlled Nafion-humidifier [55, 56] (Perma Pure PD-100T-24, with de-ionized water humidification) was used to control the RH of the sample. A measured humidogram of extinction coefficients under different RH is shown in Fig. 6.

The hygroscopic growth factor of particle diameter, GF(RH), can be calculated according to [11]:

$$GF(RH) = \frac{D(RH)}{D(Dry)}. \qquad (6)$$

where D(RH) is the mobility diameter of AS at a specific RH, and D(Dry) is the dry diameter. GF(RH) represents the relative increase in the mobility diameter due to the water uptake at a specific RH, and in this work, the values of GF(RH) under different RH were calculated with Extended Aerosol Inorganics Model (E-AIM) [57] for further application in the model calculation of the optical growth factor, f(RH) [11]:

$$f(RH) = \frac{N_{RH}Q_{ext,RH}}{N_{Dry}Q_{ext,Dry}}GF^2. \qquad (7)$$

The extinction efficiency of dry ($Q_{ext,dry}$) and humidified ($Q_{ext,RH}$) AS can be calculated by using Mie theory with the CRI value of AS, and wet particles ($m_{wet,AS}$), respectively. $m_{wet,AS}$, the volume weighted CRI, can be calculated using the volume weighted mixing rule with CRI values of m_{AS} = 1.538 + i 0 [43], and m_w = 1.335 + i 0 [11] for AS and water, respectively [11]:

$$m_{wet,AS} = \frac{D_{Dry}^3 \times m_{AS} - (D_{RH}^3 - D_{Dry}^3)\times m_w}{D_{RH}^3}. \qquad (8)$$

As shown in Fig. 6, the measured values agreed well with the modeled f(RH) values. The abrupt increase in extinction is caused by the deliquescence of AS particles. The measured deliquescence point of AS agreed well with the value reported by Bremet al. [10] using an extinction cell. The measured f(RH= 80%) of 3.8 also agreed well with the reported value of 3.7 at λ = 532 nm by Flores et al. [11]. In general, the results demonstrated that the newly-developed IBBCEAS aerosol extinction spectrometer provides a high quantity measurement of f(RH).

3.3. Ambient Measurements

Field application of the instrument was carried out for demonstration purposes at the Hefei Radiation Observatory (HeRO) site (31.90°N, 117.17°E) [58, 59] during the period of 2 Nov. to 5 Nov. 2015. The instruments were installed in a temperature controlled room (the temperature inside the extinction spectrometer enclosure was maintained at 25.6 ± 0.2 °C), with the sample inlet about 1 m above the roof. The inlet consisted of a $PM_{1.0}$ ambient size cut (SF-PM1.0, Sven Lecker Ingenieurburo GmbH) with a 50% cut point at 1.0 μm. The sample air was dried to below 20% by using a diffusion drier, and then was divided into 3 channels : the first channel was used for the size distribution measurement with a scanning mobility particle sizer (SMPS) with a time resolution of 2 min; the second channel was used to measure the dry extinction coefficient at λ = 461 nm with the previously developed cavity-enhanced aerosol albedometer [44, 45]; and the third channel was used to measure the extinction of the wet particles with the IBBCEAS aerosol extinction spectrometer. The system was operated in constant humidity mode. The RH of the wet sample was maintained at 85%. The extinction growth factor at λ = 461 nm thus can be obtained directly from the ratio of the wet and dry channel.

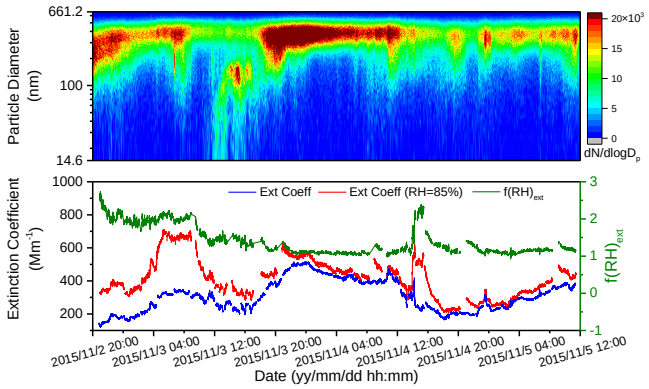

Fig. 7. Upper panel : time series of the aerosol number size distribution of dry $PM_{1.0}$ particles measured by SMPS. Lower panel : extinction coefficient of dry $PM_{1.0}$ sample, 85% RH humidified sample, and the extinction enhancement factor (*f*(RH)).

Figure 7 shows the temporal variations of the size distribution and the optical properties. The dry and wet extinction coefficients varied with the particle number concentrations, however, the *f*(RH) showed a rather different pattern. For example, large *f*(RH) values were observed on the afternoon of November 4th (a declining state of haze, and the corresponding particle number concentration also decreased). These observations suggest that the chemical composition may play an important role in the hygroscopic growth of extinction coefficient.

4. CONCLUSION

In this paper, we report the development of an IBBCEAS-based aerosol extinction spectrometer for highly sensitive and accurate measurement of aerosol extinction coefficient at λ = 461 nm. The performance evaluation of the developed instrument was tested with laboratory-generated monodispersed PSL, and the retrieved CRI agreed well with literature values. The suitability of the IBBCEAS extinction spectrometer for optical hygroscopic growth was tested with laboratory-generated AS aerosol. The measured results agreed well with the modeled *f*(RH) values. The instrument was further deployed in field measurements. These results demonstrated that the IBBCEAS-based extinction spectrometer provides a valuable method for high quality measurements of aerosol extinction coefficient and hygroscopic growth of extinction coefficient at high RH condition.

Funding Information. The China Special Fund for Meteorological Research in the Public Interest (GYHY201406039); National Natural Science Foundation of China (41330424); the Natural Science Foundation of Anhui Province (1508085J03); the Youth Innovation Promotion Association CAS (2016383).

Acknowledgment. We thank Prof. Peng Yan at Meteorological Observation Center of Chinese Academy of Meteorological Sciencefor helpful discussion.

References

1. Q. Zhang, K. He, and H.Huo, “Cleaning China's air", Nature 484, 161–162 (2012).
2. P. A. Baron, P. Kulkarni, K. Willeke, "Aerosol measurement : principles, techniques, and applications," 3rd ed., John Wiley & Sons, Inc., Hoboken, New Jersey, 2011.
3. P. H. McMurry, "A review of atmospheric aerosol measurements," Atmos. Environ. 34, 1959-1999 (2000).
4. J.C. Chow, "Measurement methods to determine compliance with ambient air quality standards for suspended particles," J. Air Waste Manage. Assoc. 45, 320-382 (1995).
5. J. G. Watson, “Visibility: Science and regulation,” J. Air Waste Manage. Assoc. 52, 628-713 (2002).
6. L. Li, J. Chen, H. Chen, X. Yang, Y. Tang, R. Zhang, "Monitoring optical properties of aerosols with cavity ring-down spectroscopy," J. Aerosol Sci. 42, 277-284 (2011).
7. P. Zieger, R. Fierz-Schmidhauser, E. Weingartner, and U. Baltensperger, "Effects of relative humidity on aerosol light scattering: results from different European sites," Atmos. Chem. Phys. 13, 10609-10631 (2013).
8. G. Titos, A. Jefferson, P. J. Sheridan, E. Andrews, H. Lyamani, L. Alados-Arboledas, and J. A. Ogren, "Aerosol light-scattering enhancement due to water uptake during the TCAP campaign," Atmos. Chem. Phys. 14, 7031-7043 (2014).
9. X. L. Pan, P. Yan, J. Tang, J. Z. Ma, Z. F. Wang, A. Gbaguidi, and Y. L. Sun, "Observational study of influence of aerosol hygroscopic growth on scattering coefficient over rural area near Beijing mega-city," Atmos. Chem. Phys. 9, 7519-7530 (2009).
10. B. T. Brem , F. C. M. Gonzalez , S. R. Meyers , T. C. Bond, and M. J. Rood, "Laboratory-measured optical properties of inorganic and organic aerosols at relative humidities up to 95%," Aerosol Sci. Tech. 46, 178-190 (2012).
11. J. M. Flores, R. Z. Bar-Or, N. Bluvshtein, A. Abo-Riziq , A. Kostinski , S. Borrmann, I. Koren, I. Koren, and Y. Rudich, "Absorbing aerosols at high relative humidity: linking hygroscopic growth to optical properties," Atmos. Chem. Phys. 12, 5511-5521 (2012).
12. R. Zhang, A. F. Khalizov, J. Pagels, D. Zhang, H. Xue, and P. H. McMurry, “Variability in morphology, hygroscopicity, and optical properties of soot aerosols during atmospheric processing,” P. Natl. Acad. Sci. USA 105, 10291–10296 (2008).
13. M. Schnaiter, O. Schmid , A. Petzold , L. Fritzsche , K. F. Klein , M. O. Andreae , G. Helas , A. Thielmann , M. Gimmler , O. Möhler , C. Linke, and U. Schurath, “Measurement of Wavelength-Resolved Light Absorption by Aerosols Utilizing a UV-VIS Extinction Cell,” Aerosol Sci. Tech. 39, 249-260 (2005).
14. A. Virkkula, N. Ahlquist, D. Covert, P. Sheridan, W. Arnott, and J. Ogren, “A three-wavelength optical extinction cell for measuring aerosol light extinction and its application to determining light absorption coefficient,” Aerosol Sci. Tech. 39, 52–67 (2005).

15. M. Schnaiter, H. Horvath, O. Möhler, K. H. Naumann, H. Saathoff, and O. W. Schöck, "UV-VIS-NIR spectral optical properties of soot and soot-containing aerosols," J. Aerosol Sci. 34, 1421–1444 (2003).
16. R. T. Chartier, and M. E. Greenslade, "Initial investigation of the wavelength dependence of optical properties measured with a new multi-pass Aerosol Extinction Differential Optical Absorption Spectrometer (AE-DOAS)," Atmos. Meas. Tech. 5, 709–721 (2012).
17. C. E. Jordan, B. E. Anderson, A. J. Beyersdorf, C. A. Corr, J. E. Dibb, M. E. Greenslade, R. F. Martin, R. H. Moore, E. Scheuer, M. A. Shook, K. L. Thornhill, D. Troop, E. L. Winstead, and L. D. Ziemba, "Spectral aerosol extinction (SpEx): a new instrument for in situ ambient aerosol extinction measurements across the UV/visible wavelength range," Atmos. Meas. Tech. 8, 4755-4771 (2015).
18. A. D. Sappey, E. S. Hill, T. Settersten, and M. A. Linne, "Fixed-frequency cavity ringdown diagnostic for atmospheric particulate matter," Opt. Lett. 23, 954–956 (1998).
19. J. D. Smith, and D. B. Atkinson, "A portable pulsed cavity ring-down transmissometer for measurement of the optical extinction of the atmospheric aerosol," Analyst 126, 1216–1220 (2001).
20. J. E. Thompson, B. W. Smith, and J. D. Winefordner, "Monitoring atmospheric particulate matter through cavity ring-down spectroscopy," Anal. Chem. 74, 1962–1967 (2002).
21. A. Pettersson, E. R. Lovejoy, C. A. Brock, S. S. Brown, and A. R. Ravishankara, "Measurement of aerosol optical extinction at 532 nm with pulsed cavity ring down spectroscopy," J. Aerosol Sci. 35, 995–1011 (2004).
22. J. E. Thompson, and H. D. Spangler, "Tungsten source integrated cavity output spectroscopy for the determination of ambient atmospheric extinction coefficient," Appl. Optics, 45 2465–2473 (2006).
23. P. L. Kebabian, W. A. Robinson, and A. Freedman, "Optical extinction monitor using cw cavity enhanced detection," Rev. Sci. Instrum. 78, 063102 (2007).
24. A. Abo Riziq, C. Erlick, E. Dinar, and Y. Rudich, "Optical properties of absorbing and non-absorbing aerosols retrieved by cavity ring down (CRD) spectroscopy," Atmos. Chem. Phys. 7, 1523–1536 (2007).
25. P. L. Kebabian, W. A. Robinson, and A. Freedman, "Optical extinction monitor using cw cavity enhanced detection," Rev. Sci. Instrum. 78, 063102 (2007).
26. N. Lang-Yona, Y. Rudich, E. Segre, E. Dinar, and A. Abo-Riziq, "Complex refractive indices of aerosols retrieved by continuous wave-cavity ring down aerosol spectrometer," Anal. Chem. 81, 1762–1769 (2009).
27. P. Massoli, P. L. Kebabian, T. B. Onasch, F. B. Hills, and A. Freedman, "Aerosol light extinction measurements by Cavity Attenuated Phase Shift (CAPS) spectroscopy: laboratory validation and field deployment of a compact aerosol particle extinction monitor," Aerosol Sci. Tech. 44, 428–435 (2010).
28. D. Mellon, S. J. King, J. Kim, J. P. Reid, and A. J. Orr-Ewing, "Measurements of extinction by aerosol particles in the nearinfrared using continuous wave cavity ring-down spectroscopy," J. Phys. Chem. A 115, 774–783 (2011).
29. N. Bluvshtein, J. M. Flores, A. A. Riziq, and Y. Rudich, "An approach for faster retrieval of aerosols' complex refractive index using cavity ring-down spectroscopy," Aerosol Sci. Tech. 46, 1140–1150 (2012).
30. L. Wang, W. Wang, and M. Ge, "Extinction efficiencies of mixed aerosols measured by aerosol cavity ring down spectrometry," Chinese Sci. Bull. 57, 2567–2573 (2012).
31. A. Petzold, T. Onasch, P. Kebabian, and A. Freedman, "Intercomparison of a Cavity Attenuated Phase Shift-based extinction monitor (CAPS PMex) with an integrating nephelometer and a filter-based absorption monitor," Atmos. Meas. Tech. 6, 1141–1151 (2013).
32. T. D. Gordon, N. L. Wagner, M. S. Richardson, D. C. Law, D. Wolfe, E. W. Eloranta, C. A. Brock, F. Erdesz, D. M. Murphy, "Design of a novel open-path aerosol extinction cavity ringdown spectrometer," Aerosol Sci. Tech. 49, 716-725 (2015).
33. H. Moosmüller, R. K. Chakrabarty, and W. P. Arnott, "Aerosol light absorption and its measurement," J. Quant. Spectrosc. Radiat. Transfer 110, 844 - 878 (2009).
34. A. Laskin, J. Laskin, and S. A. Nizkorodov, "Chemistry of atmospheric brown carbon," Chem. Rev. 115, 4335 - 4382 (2015).
35. T. Moise, J. M. Flores, and Y. Rudich, "Optical properties of secondary organic aerosols and their changes by chemical processes," Chem. Rev. 115, 4400 - 4439 (2015).
36. S. S. Brown, "Absorption spectroscopy in high-finesse cavity for atmospheric studies," Chem. Rev. 103, 5219–5238 (2003).
37. J. M. Langridge, M. S. Richardson, D. Lack, D. Law, and D. M. Murphy, "Aircraft instrument for comprehensive characterization of aerosol optical properties, Part I: wavelength-dependent optical extinction and its relative humidity dependence measured using cavity ringdown spectroscopy," Aerosol Sci. Tech. 45, 1305 - 1318 (2011).
38. S. E.Fiedler , A. Hese, and A. A. Ruth, "Incoherent broad-band cavity-enhanced absorption spectroscopy," Chem. Phys. Lett. 371, 284–294 (2003).
39. A. A. Ruth, S. Dixneuf, and R. Raghunandan, " Broadband Cavity-Enhanced Absorption Spectroscopy with Incoherent Light" Editors: G. Gagliardi, and H.-P. Loock, "Cavity-enhanced spectroscopy and sensing," Volume 179 of the series Springer Series in Optical Sciences pp 485-517 (2014).
40. R. M. Varma, D. S. Venables, A. A. Ruth, U. Heitmann, E. Schlosser, and S. Dixneuf, "Long optical cavities for open-path monitoring of atmospheric trace gases and aerosol extinction, " App. Opt. 48, B159-B171 (2009).
41. R. M. Varma, S. M. Ball, T. Brauers, H.-P. Dorn, U. Heitmann, J R. L. ones, Platt, D. Pöhler, A. A. Ruth, A. J. L. Shillings, J. Thieser, A. Wahner, and D. S. Venables, "Light extinction by secondary organic aerosol: an intercomparison of three broadband cavity spectrometers," Atmos. Meas. Tech. 6, 3115-3130 (2013).
42. R. Thalman, and R. Volkamer, "Inherent calibration of a blue LED-CE-DOAS instrument to measure iodine oxide, glyoxal, methyl glyoxal, nitrogen dioxide, water vapour and aerosol extinction in open cavity mode," Atmos. Meas. Tech. 3, 1797–1814 (2010).
43. W. Zhao, M. Dong, W. Chen, X. Gu, C. Hu, X. Gao, W. Huang, W. Zhang, "Wavelength-resolved optical extinction measurements of aerosols using broad-band cavity-enhanced absorption spectroscopy over the spectral range of 445 - 480 nm," Anal. Chem. 85, 2260-2268 (2013).
44. W. Zhao, X. Xu, M. Dong, W. Chen, X. Gu, C. Hu, Y. Huang, X. Gao, W. Huang, and W. Zhang, "Development of a cavity-enhanced aerosol albedometer," Atmos. Meas. Tech. 7, 2551-2566 (2014).
45. X. Xu, W. Zhao, Q. Zhang, S. Wang, B. Fang, W. Chen, D. S. Venables, X. Wang, W. Pu, X. Wang, X. Gao, and W. Zhang, "Optical properties of atmospheric fine particles near Beijing during the HOPE-J^{3}A campaign," Atmos. Chem. Phys. 16, 6421-6439 (2016).
46. R. A. Washenfelder, J. M. Flores, C. A. Brock, S. S. Brown, and Y. Rudich, "Broadband measurements of aerosol extinction in the ultraviolet spectral region," Atmos. Meas. Tech., 6, 861 - 877 (2013).
47. J. M. Flores, R. A. Washenfelder, G. Adler, H. J. Lee, L. Segev, J. Laskin, A. Laskin, S. A. Nizkorodov, S. S. Brown and Y. Rudich, "Complex refractive indices in the near-ultraviolet spectral region of biogenic secondary organic aerosol aged with ammonia," Phys. Chem. Chem. Phys. 16, 10629 - 10642 (2014).
48. J. M. Flores, D. F. Zhao, L. Segev, P. Schlag, A. Kiendler-Scharr, H. Fuchs, Å. K. Watne, N. Bluvshtein, Th. F. Mentel, M. Hallquist, and Y. Rudich, "Evolution of the complex refractive index in the UV spectral region in ageing secondary organic aerosol," Atmos. Chem. Phys. 14, 5793–5806 (2014).
49. N. Bluvshtein, J. M. Flores, L. Segev, and Y. Rudich, "A new approach for retrieving the UV–vis optical properties of ambient aerosols," Atmos. Meas. Tech. 9, 3477–3490 (2016).
50. R. A. Washenfelder, A. O. Langford, H. Fuchs, and S. S. Brown, "Measurement of glyoxal using an incoherent broadband cavity

enhanced absorption spectrometer," Atmos. Chem. Phys. 8, 7779-7793 (2008).
51. H. Naus, and W. Ubachs, "Experimental verification of Rayleigh scattering cross sections," Opt. Lett. 25, 347–349 (2000).
52. M. Sneep, and W. Ubachs, "Direct measurement of the Rayleigh scattering cross section in various gases," J. Quant. Spectrosc. Radiat. Transfer 92, 293–310 (2005).
53. Y. Chen, C. Yang, W. Zhao, B. Fang, X. Xu, Y. Gai, X. Lin, W. Chen, W. Zhang, "Ultra-sensitive measurement of peroxy radicals by chemical amplification broadband cavity-enhanced spectroscopy," Analyst 141, 5870 – 5878 (2016).
54. N. Lang-Yona, Y. Rudich, E. Segre, E. Dinar, and A. Abo-Riziq, "Complex refractive indices of aerosols retrieved by continuous wave-cavity ring down aerosol spectrometer,"Anal. Chem. 81, 1762–1769 (2009).
55. R. Fierz-Schmidhauser, P. Zieger, G. Wehrle, A. Jefferson, J. A. Ogren, U. Baltensperger, and E. Weingartner, "Measurement of relative humidity dependent light scattering of aerosols," Atmos. Meas. Tech. 3, 39-50 (2010).
56. J. M. Langridge, M. S. Richardson , D. A. Lack , C. A. Brock, D. M. Murphy, "Limitations of the photoacoustic technique for aerosol absorption measurement at high relative humidity," Aerosol Sci. Tech. 47, 1163-1173 (2013).
57. A. S.Wexler, and S. L. Clegg, "Atmospheric aerosol models for systems including the ions H^+, NH_4^+, Na^+, SO_4^{2-}, NO_3^-, Cl^-, Br^-, and H_2O," J. Geophys. Res. 107, ACH 14-1 - ACH 14-14(2002).
58. X. Zhang, Y. Huang, R.Rao, and Z. Wang, "Retrieval of effective complex refractive indexfrom intensive measurements of characteristics of ambient aerosols in the boundary layer,"Opt. Express 21, 17849-17862 (2013).
59. Z.Wang, D. Liu, Z. Wang, Y. Wang, P. Khatri, J. Zhou, T. Takamura, and G. Shi, "Seasonal characteristics of aerosol optical properties at the SKYNET Hefei site (31.90°N, 117.17°E) from 2007 to 2013," J. Geophys. Res. Atmos. 119, 6128–6139 (2014).